




Double rapid adiabatic passage in three optical waveguides with longitudinally varying detuningsJian Chen , Li Deng ,* Yueping Niu , and Shangqing Gong*Department of Physics, East China University of Science and Technology, Shanghai 200237, China*

(Received 9 February 2021; revised 28 April 2021; accepted 3 May 2021; published 11 May 2021)

In this paper, optical simulation of double rapid adiabatic passage (RAP) is investigated in three evanescently coupled waveguides with longitudinally varying detunings of the propagation constants. Unlike the time-dependent detuning which is kept linearly increased or decreased when the RAP is applied in two-state atomic systems, here all possible situations of the corresponding space-dependent detunings with or without sign flips are considered. At the maximum of the couplings in the waveguide structure, the detunings tend to become zero and the sign flips are supposed to occur. Theoretical analysis shows that different light evolutions such as light splitting, complete light transfer, or complete light return can be realized adiabatically, depending on the choices of the detunings. Moreover, two of the above three phenomena can be observed simultaneously in the waveguide structure under some circumstances. The theoretical analysis is confirmed by numerical calculations. Due to the robustness of the double RAP, the technique can be applied to design optical devices such as achromatic beam splitters or beam couplers.

DOI: [10.1103/PhysRevA.103.053705](https://doi.org/10.1103/PhysRevA.103.053705)**I. INTRODUCTION**

In recent years, interest in directly applying quantum control techniques such as Landau-Zener tunneling [1], electromagnetically induced transparency, Autler-Townes splitting [2], and adiabatic elimination [3,4] in optical waveguides has grown rapidly. It originates from the mathematical similarity between the time-dependent Schrödinger equation and the optical wave equation describing the spatial propagation of monochromatic light in dielectric structures. Classical analogs of quantum dynamics in optical waveguides has now become a hot topic and the reasons are the following [5]: First, optical waveguides provide a direct and easy visualization in space of typical ultrafast phenomena in time; second, optical waveguides are good platforms to explore coherent dynamical regimes not yet accessible in atomic systems. Furthermore, such classical analogs have found important applications in compact photonic devices [3].

Among those quantum control techniques which have been optically simulated, adiabatic passages such as the rapid adiabatic passage (RAP) and the stimulated Raman adiabatic passage were most investigated in optical waveguides [6–19]. This is because adiabatic passages in atomic systems are intrinsically robust and they can take place over a wide range of the parameters of the incident pulses. Correspondingly, requirements toward the design parameters of the optical waveguides can be greatly relaxed when carrying out classical analogs of the adiabatic passages. Therefore, adiabatic passages were usually applied to design optical devices with stable performances [13,14,16,17]. What is more, the lengths of the optical waveguides required by the adiabatic passages can be further shortened while the adiabaticity is

still preserved [20–27]. This is achieved with the help of the “shortcuts to adiabaticity” technique, which was originally introduced to speed up the adiabatic processes in atomic systems.

Despite the similarities between the atomic systems and optical waveguides, it is important to note that there is a conceptual difference between them. As for the atomic states, the population decrease is generally unavoidable due to the dephasing effects. However, it is not the case for the optical waveguides. Light loss in optical waveguides can be negligible under certain conditions. Such a difference inspires us that, when borrowing quantum control techniques for the design of optical devices, not only those which are physically interesting like mentioned above can be employed, those which lack interest in quantum physics can also be borrowed to design devices with new functionalities in optical waveguides.

Based on the above idea, we are going to study an extension of the RAP in optical waveguides in this paper. The RAP is a well-known adiabatic process in a two-state system which can completely transfer the population from the ground state into the excited state by a linearly chirped pulse. When extending the use of the RAP in a three-state system with two chirped pulses, which is a “double RAP” process, it may also lead to complete population transfer or coherent superposition of the three states. However, such a technique in atomic systems more or less lacks interest in quantum physics. The reasons are mainly the following: On one hand, the population should be located in the ground state at the beginning since it is not true if the population initially locates in the excited states. On the other hand, it is also not interesting if a coherent superposition state is generated between the excited states because it vanishes rapidly due to the dephasing effects. In contrast, we do not encounter these problems when carrying out the classical analog of the double RAP in optical waveguides. First, light can be incident into any one of the

*dengli@ecust.edu.cn

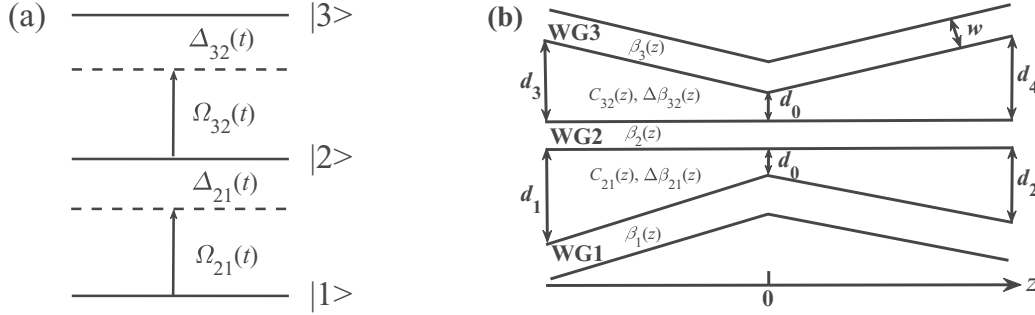


FIG. 1. (a) Schematic diagram of double RAP in a ladder-type three-state system where two linearly chirped pulses are employed. $\Omega_{jm}(t)$ and $\Delta_{jm}(t)$ ($j, m = 1, 2, 3$) are the time-dependent Rabi frequency and detuning, respectively. (b) Optical simulation of the double RAP in three evanescently coupled waveguides, where $C_{jm}(z)$ and $\Delta\beta_{jm}(z)$ ($j, m = 1, 2, 3$) are the space-dependent coupling constant and detuning, respectively. $\beta_j(z)$ ($j = 1, 2, 3$) and w are the propagation constant and width of the waveguide, while d_j ($j = 0, 1, 2, 3, 4$) is the distance between the adjacent waveguides.

waveguides, which correspond to the atomic states, with no priority. Second, it is meaningful if we observe light transfer or light splitting in waveguides, since the light loss can reasonably be ignored. Therefore, we consider that the study of double RAP in optical waveguides is still of interest and may help us design new optical devices.

We will directly discuss the light propagation in three evanescently coupled waveguides under the double RAP by analyzing the “eigenstates” of the coupling matrix of the coupled mode equations. Since the spatial detuning comes from the difference between the propagation constants of the waveguides and can be manipulated with more freedom than the temporal detuning [28,29], all possible situations of the spatially varying detunings along the propagation direction with or without sign flips are investigated. The sign flips are supposed to occur at the position where the spatial detunings tend to be zero and the couplings between the waveguides are increased to their maximum. Note that similar treatment has been used in Ref. [18] where the light evolution in a three-waveguide structure was predicted based on the adiabatic “eigenstates” in the case where the positions of maximum coupling and zero detuning do not correspond. Based on the double RAP, theoretical analysis predicts some spatial adiabatic passages such as light splitting, complete light transfer, or complete light return under different choices of the detunings. What is more, it is found that two of the above three phenomena can be observed simultaneously in the waveguide structure in some cases. Numerical calculations by directly solving the coupled mode equations and optical simulations based on the beam propagation method (BPM) are in good agreement with the theoretical predictions. The double RAP can have possible applications in optical waveguides for the design of achromatic beam splitters or beam couplers due to its robustness.

II. THEORETICAL ANALYSIS

We start by considering a ladder-type three-state system as shown in Fig. 1(a). The double RAP occurs when two linearly chirped pulses interact with such a system. In this figure, $\Omega_{jm}(t)$ and $\Delta_{jm}(t)$ ($j, m = 1, 2, 3$) are the time-dependent Rabi frequency and detuning. As for the optical simulation of the double RAP, three evanescently coupled waveguides

as illustrated in Fig. 1(b) are demanded. The distance d_j ($j = 0, 1, 2, 3, 4$) between the adjacent waveguides and the propagation constant $\beta_j(z)$ ($j = 1, 2, 3$) are supposed to vary along the propagation direction. Consequently, we can obtain the space-dependent coupling constant $C_{jm}(z)$ and detuning $\Delta\beta_{jm}(z)$ ($j, m = 1, 2, 3$), which mimic the time-dependent Rabi frequency $\Omega_{jm}(t)$ and detuning $\Delta_{jm}(t)$, respectively. The propagation of the optical fields in waveguide structure displayed in Fig. 1(b) can then be described by the coupled mode theory [30],

$$\begin{aligned} i\frac{d}{dz}a_1 &= \beta_1(z)a_1 + k_{12}(z)a_2 \\ i\frac{d}{dz}a_2 &= \beta_2(z)a_2 + k_{21}(z)a_1 + k_{23}(z)a_3 \\ i\frac{d}{dz}a_3 &= \beta_3(z)a_3 + k_{32}(z)a_2, \end{aligned} \quad (1)$$

where a_j ($j = 1, 2, 3$) is the electric field amplitude of the wave traveling in three waveguides. $k_{jm}(z)$ ($j, m = 1, 2, 3$) is the coupling coefficient from waveguide m (WG m) to waveguide j (WG j). Generally, $k_{jm}(z) \neq k_{mj}(z)$ unless the two waveguides are identical to each other. By setting $a_j = a'_j e^{-i\beta_j(z)z}$, the above equation can be further written in the following:

$$\begin{aligned} i\frac{d}{dz}\begin{pmatrix} a'_1 \\ a'_2 \\ a'_3 \end{pmatrix} &= \begin{pmatrix} 0 & k_{12}(z)e^{-i\Delta\beta_{21}(z)z} & 0 \\ k_{21}(z)e^{i\Delta\beta_{21}(z)z} & 0 & k_{23}(z)e^{-i\Delta\beta_{32}(z)z} \\ 0 & k_{32}(z)e^{i\Delta\beta_{32}(z)z} & 0 \end{pmatrix} \\ &\times \begin{pmatrix} a'_1 \\ a'_2 \\ a'_3 \end{pmatrix}, \end{aligned} \quad (2)$$

in which the detuning $\Delta\beta_{jm}(z)$ is defined as $\Delta\beta_{jm}(z) = \beta_j(z) - \beta_m(z)$ ($j, m = 1, 2, 3$). We can continue to perform the transformation by setting $b_1 = \sqrt{k_{21}(z)/k_{12}(z)}a'_1$, $b_2 = a'_2 e^{-i\Delta\beta_{21}(z)z}$ and $b_3 = \sqrt{k_{23}(z)/k_{32}(z)}a'_3 e^{i\Delta\beta_{31}(z)z}$, and

we obtain that

$$i \frac{d}{dz} \begin{pmatrix} b_1 \\ b_2 \\ b_3 \end{pmatrix} = \begin{pmatrix} 0 & C_{21}(z) & 0 \\ C_{21}(z) & \Delta\beta_{21}(z) & C_{32}(z) \\ 0 & C_{32}(z) & \Delta\beta_{31}(z) \end{pmatrix} \begin{pmatrix} b_1 \\ b_2 \\ b_3 \end{pmatrix}. \quad (3)$$

In this equation, the coupling constants $C_{21}(z) = \sqrt{k_{12}(z)k_{21}(z)}$ and $C_{32}(z) = \sqrt{k_{23}(z)k_{32}(z)}$ are defined as the geometrical averages of the above coefficients $k_{jm}(z)$, respectively.

By mapping the longitudinal z dependence into time dependence, we can clearly see that Eq. (3) is identical to the time-dependent Schrödinger equation which describes the light-matter interaction as depicted in Fig. 1(a). The 3×3 matrix in Eq. (3), which we call the ‘‘coupling matrix’’, corresponds to the Hamiltonian in the Schrödinger equation. The coupling constant $C_{jm}(z)$ corresponds to the Rabi frequency $\Omega_{jm}(t)$, while the longitudinally varying detuning $\Delta\beta_{jm}(z)$ corresponds to the time-dependent detuning $\Delta_{jm}(t)$. Therefore, the spatial dynamics of coupled waveguides are analogous to the temporal dynamics of atomic systems.

As we know, it is quite an effective method to predict the evolution of the atomic system by analyzing the eigenstates of the Hamiltonian. Likewise, the treatment can also be very helpful to understand the dynamics in optical waveguides. Hence, we are going to calculate the ‘‘eigenstates’’ of the coupling matrix in Eq. (3) for discussing the light propagation in the three coupled waveguides. However, we find that a general solution of the coupling matrix with such a form is difficult to be obtained. The ‘‘eigenstates’’ can only be achieved under some special circumstances of the matrix. For this reason, we simply assume here that the two coupling constants are equal with each other, which is $C_{21}(z) = C_{32}(z) = C(z)$. In addition, the detuning between WG1 and WG3 is chosen with two special values, which are $\Delta\beta_{31}(z) = 0$ and $\Delta\beta_{31}(z) = 2\Delta\beta_{21}(z)$, respectively. In the following, we will first calculate the ‘‘eigenstates’’ of the coupling matrix under the above assumptions. Then we will discuss the evolution of light in optical waveguides based on the calculated ‘‘eigenstates’’ under the double RAP.

For the first special choice with $\Delta\beta_{31}(z) = 0$, the two detunings, $\Delta\beta_{32}(z)$ and $\Delta\beta_{21}(z)$, satisfy the relation $\Delta\beta_{32}(z) = -\Delta\beta_{21}(z)$ due to the definition of $\Delta\beta_{31}(z)$, which is $\Delta\beta_{31}(z) = \Delta\beta_{32}(z) + \Delta\beta_{21}(z)$. In this case, the eigenvalues and the corresponding ‘‘eigenstates’’ of the coupling matrix can be easily obtained [31], which are

$$\begin{aligned} \varepsilon_1^+ &= \frac{\Delta\beta_{21}(z) + \sqrt{\Delta\beta_{21}^2(z) + 8C^2(z)}}{2} \\ \varepsilon_1 &= 0 \\ \varepsilon_1^- &= \frac{\Delta\beta_{21}(z) - \sqrt{\Delta\beta_{21}^2(z) + 8C^2(z)}}{2} \end{aligned} \quad (4)$$

and

$$\begin{aligned} \Psi_1^+(z) &= \frac{\sqrt{2}}{2} \sin\gamma b_1 + \cos\gamma b_2 + \frac{\sqrt{2}}{2} \sin\gamma b_3 \\ \Psi_1(z) &= \frac{\sqrt{2}}{2} b_1 - \frac{\sqrt{2}}{2} b_3 \end{aligned}$$

$$\begin{aligned} \Psi_1^-(z) &= \frac{\sqrt{2}}{2} \cos\gamma b_1 - \sin\gamma b_2 \\ &+ \frac{\sqrt{2}}{2} \cos\gamma b_3, \end{aligned} \quad (5)$$

respectively. In Eq. (5), the mixing angle γ is defined as $\tan 2\gamma = \frac{2\sqrt{2}C(z)}{\Delta\beta_{21}(z)}$.

As for the second special choice with $\Delta\beta_{31}(z) = 2\Delta\beta_{21}(z)$, the two detunings between adjacent waveguides now satisfy $\Delta\beta_{32}(z) = \Delta\beta_{21}(z)$. In this case, the calculation becomes much more complicated. Nevertheless, we can still obtain the ‘‘eigenstates’’ with analytical expressions. The eigenvalues of the coupling matrix can be written as

$$\begin{aligned} \varepsilon_2^+ &= \Delta\beta_{21}(z) + C'(z) \\ \varepsilon_2 &= \Delta\beta_{21}(z) \\ \varepsilon_2^- &= \Delta\beta_{21}(z) - C'(z), \end{aligned} \quad (6)$$

where the parameter $C'(z)$ is defined as $C'(z) = \sqrt{\Delta\beta_{21}^2(z) + 2C^2(z)}$. Correspondingly, the ‘‘eigenstates’’ of the coupling matrix have the following form:

$$\begin{aligned} \Psi_2^+(z) &= \frac{\sqrt{1 + \cos^2\theta}}{\sqrt{2}} \sin\varphi b_1 + \frac{\sin\theta}{\sqrt{2}} b_2 \\ &+ \frac{\sqrt{1 + \cos^2\theta}}{\sqrt{2}} \cos\varphi b_3 \\ \Psi_2(z) &= \frac{\sqrt{2}}{2} \sin\theta b_1 + \cos\theta b_2 - \frac{\sqrt{2}}{2} \sin\theta b_3 \\ \Psi_2^-(z) &= -\frac{\sqrt{1 + \cos^2\theta}}{\sqrt{2}} \cos\varphi b_1 + \frac{\sin\theta}{\sqrt{2}} b_2 \\ &- \frac{\sqrt{1 + \cos^2\theta}}{\sqrt{2}} \sin\varphi b_3, \end{aligned} \quad (7)$$

in which the two mixing angles, θ and φ , are defined as $\tan\theta = \frac{\sqrt{2}C(z)}{\Delta\beta_{21}(z)}$ and $\tan\varphi = \frac{C'(z) - \Delta\beta_{21}(z)}{C'(z) + \Delta\beta_{21}(z)}$, respectively.

According to the above ‘‘eigenstates’’ given in Eqs. (5) and (7), we can proceed to discuss the evolution of light in the three coupled waveguides under the double RAP. Note that the adiabatic condition must be fulfilled for the adiabatic passage to occur, which is

$$\left| \left\langle \frac{d\Psi_j}{dz} \middle| \Psi_j^\pm \right\rangle \right| \ll |\varepsilon_j - \varepsilon_j^\pm| (j = 1, 2). \quad (8)$$

Generally speaking, the adiabatic condition requires that the coupling constants and the detunings should vary smoothly.

In the framework of the double RAP, the variations of the two identical coupling constants, $C_{32}(z)$ and $C_{21}(z)$, are accordant with what is depicted in Fig. 1(b). At the central position of the structure, which is $z = 0$, the adjacent waveguides have minimum distances and corresponding maximum couplings. Theoretically, the waveguide lengths in Fig. 1(b) are supposed to be infinitely long. Therefore, the couplings at the inputs and outputs of the waveguides can be safely ignored.

As for the two spatially varying detunings, $\Delta\beta_{32}(z)$ and $\Delta\beta_{21}(z)$, they are supposed to be linearly varied along the propagation direction. In addition, the two detunings can have

sign flips or not. Therefore, the two detunings can be written as $\Delta\beta_{jm}(z) = \pm\alpha z$ or $\Delta\beta_{jm}(z) = \pm|\alpha z|$ with α the positive “linear chirp rate”. The expression implies that the absolute values of the two detunings, $|\Delta\beta_{jm}(z)|$, reach their maximum at the inputs and outputs of the waveguides. The two detunings tend to be zero at $z = 0$ where the sign flips may appear.

Since there are many possibilities of the two longitudinally varying detunings, various light evolutions in the waveguide structure can be expected. Thus we are going to investigate all possible situations in the following subsections.

A. Sign flips in both detunings

We first consider the situation that both longitudinally varying detunings have sign flips, which is $\Delta\beta_{32}(z) = \pm\alpha z$ and $\Delta\beta_{21}(z) = \pm\alpha z$. In this situation, the two detunings can increase (decrease) simultaneously along the propagation direction or they can vary oppositely. Since the same or the opposite variations of the two detunings may lead to different light propagations in the waveguide structure, we should discuss the two cases separately.

1. Same variations of the two detunings

If both detunings have the same variations, which is $\Delta\beta_{32}(z) = \Delta\beta_{21}(z) = \pm\alpha z$, then it results in $\Delta\beta_{31}(z) = 2\Delta\beta_{21}(z)$. In this case, light will evolve adiabatically following the “eigenstates” in Eq. (7) as long as the adiabatic condition is satisfied.

Given $\Delta\beta_{32}(z) = \Delta\beta_{21}(z) = \alpha z$, we find that $C(z) = 0$ and $\Delta\beta_{21}(z) = -\infty$ in Eq. (7) when the light starts to propagate from $z = -\infty$. Consequently, the two mixing angles θ and φ in Eq. (7) are calculated to be π and $\frac{\pi}{2}$, respectively. When the light arrives at $z = 0$, the coupling $C(z)$ reaches its maximum and the detuning $\Delta\beta_{21}(z)$ tend to zero. At this position, the two mixing angles θ and φ gradually evolve to $\frac{\pi}{2}$ and $\frac{\pi}{4}$, respectively. When the light finally comes out from the waveguides at $z = +\infty$, the coupling $C(z)$ vanishes again and the detuning $\Delta\beta_{21}(z) = +\infty$, which leads that both mixing angles gradually become zero. According to the evolutions of the mixing angles θ and φ , the three “eigenstates” in Eq. (7) will evolve following

$$\begin{aligned}\Psi_2^+(z) : b_1 &\rightarrow \left(\frac{1}{2}b_1 + \frac{\sqrt{2}}{2}b_2 + \frac{1}{2}b_3\right) \rightarrow b_3 \\ \Psi_2(z) : -b_2 &\rightarrow \left(\frac{\sqrt{2}}{2}b_1 - \frac{\sqrt{2}}{2}b_3\right) \rightarrow b_2 \\ \Psi_2^-(z) : -b_3 &\rightarrow \left(-\frac{1}{2}b_1 + \frac{\sqrt{2}}{2}b_2 - \frac{1}{2}b_3\right) \rightarrow -b_1.\end{aligned}\quad (9)$$

Now we can predict the light propagation in waveguides from the above evolutions of the three “eigenstates”. Suppose the light is initially incident into WG1, which means that the normalized electric field amplitude $b_1 = 1$, then the light will evolve following the adiabatic state $\Psi_2^+(z)$. We can see from the adiabatic state that a “superposition state” of the three waveguides is generated at $z = 0$, indicating part of the light in WG1 is gradually coupled into WG3 through the intermediate waveguide (WG2). When the light comes out from the waveguide structure, all the light left in WG1 and WG2 is coupled

into WG3. Thus we can predict complete light transfer from WG1 to WG3. Similar is true when the light is initially incident into WG3. We can find complete light transfer from WG3 to WG1 through WG2, following the adiabatic state $\Psi_2^-(z)$. If the light starts to propagate from the intermediate waveguide, then the light will evolve adiabatically following $\Psi_2(z)$. It is found that all the light in WG2 will be coupled into the two outer waveguides WG1 and WG3 with the same intensity at position $z = 0$. However, the light in the outer waveguides will transfer back into WG2 and finally come out from this waveguide. Therefore, complete light return can be expected.

We can carry out similar analysis when $\Delta\beta_{32}(z) = \Delta\beta_{21}(z) = -\alpha z$. Complete light transfer and complete light return are also found in this case, which are just the same as those described above. Thus we do not show them here.

2. Opposite variations of the two detunings

If the two detunings along the propagation direction vary the opposite, which corresponds to $\Delta\beta_{32}(z) = -\Delta\beta_{21}(z) = \pm\alpha z$, then we find that the detuning between WG1 and WG3 satisfies $\Delta\beta_{31}(z) = 0$. Therefore, the light will propagate following the “eigenstates” in Eq. (5), provided the adiabatic condition holds. Since the analysis is the same as that in the above subsection, we will directly give the evolutions of the mixing angles and the “eigenstates” in the following.

Suppose $\Delta\beta_{32}(z) = -\Delta\beta_{21}(z) = \alpha z$, then we find that the mixing angle γ in Eq. (5) will evolve according to $0 \rightarrow \frac{\pi}{4} \rightarrow \frac{\pi}{2}$ during the light propagation from the inputs to the outputs through position $z = 0$. Correspondingly, the evolutions of the three “eigenstates” obey

$$\begin{aligned}\Psi_1^+(z) : b_2 &\rightarrow \left(\frac{1}{2}b_1 + \frac{\sqrt{2}}{2}b_2 + \frac{1}{2}b_3\right) \rightarrow \left(\frac{\sqrt{2}}{2}b_1 + \frac{\sqrt{2}}{2}b_3\right) \\ \Psi_1(z) : \frac{\sqrt{2}}{2}b_1 - \frac{\sqrt{2}}{2}b_3 & \\ \Psi_1^-(z) : \left(\frac{\sqrt{2}}{2}b_1 + \frac{\sqrt{2}}{2}b_3\right) &\rightarrow \left(\frac{1}{2}b_1 - \frac{\sqrt{2}}{2}b_2 + \frac{1}{2}b_3\right) \rightarrow -b_2.\end{aligned}\quad (10)$$

Based on the above expression, we can continue to discuss the dynamics of light in the waveguide structure. If the light is initially incident into WG2, it will be totally coupled into WG1 and WG3 with the same intensity after the propagation, as described by the adiabatic state $\Psi_1^+(z)$. Therefore, a one-to-two beam splitting can be realized. If the light is incident into WG1 at the inputs, it is found that its evolution does not follow any one of the adiabatic states in Eq. (10). Nevertheless, we note that the situation can be considered as a superposition of the adiabatic states $\Psi_1(z)$ and $\Psi_1^-(z)$, which is $b_1 = \frac{\sqrt{2}}{2}[\Psi_1(z) + \Psi_1^-(z)]$ at the inputs. Suppose the adiabatic condition holds, then the two adiabatic states $\Psi_1(z)$ and $\Psi_1^-(z)$ can evolve independently and we can still predict the light evolution. At the outputs, the adiabatic state $\Psi_1(z)$ does not change after the light propagation while $\Psi_1^-(z)$ gradually evolves into $-b_2$. Therefore, the superposition of the two adiabatic states finally evolves into $\frac{1}{2}b_1 - \frac{\sqrt{2}}{2}b_2 - \frac{1}{2}b_3$. Hence, we predict a light splitting with half of the light intensity coming out of WG2 while the left half is equally distributed between

WG1 and WG3. Similar analysis can be carried out when the light is initially incident into WG3 and the prediction is the same as that when the light starts to propagate in WG1.

As for the case when $\Delta\beta_{32}(z) = -\Delta\beta_{21}(z) = -\alpha z$, the analysis leads to the same results as those when $\Delta\beta_{32}(z) = -\Delta\beta_{21}(z) = \alpha z$. We do not describe them here for simplicity.

B. Sign flip in either one of the two detunings

Now we consider the second situation that only one of the two detunings has a sign flip. In this situation, there are still several different choices of the two detunings. First, we suppose the detuning $\Delta\beta_{32}(z)$ has no sign flip while the detuning $\Delta\beta_{21}(z)$ is still linearly varied with a sign flip, which is $\Delta\beta_{32}(z) = |\alpha z|$ and $\Delta\beta_{21}(z) = \pm\alpha z$. Since the increase or decrease of the detuning $\Delta\beta_{21}(z)$ along the propagation direction will lead to different light evolutions, we should discuss them separately.

1. Linear increase of detuning $\Delta\beta_{21}(z)$

If $\Delta\beta_{21}(z)$ is linearly increased along the propagation direction, which corresponds to $\Delta\beta_{21}(z) = \alpha z$, we can find that the detuning $\Delta\beta_{31}(z)$ satisfies the condition $\Delta\beta_{31}(z) = 0$ during the light propagation from $z = -\infty$ to $z = 0$. When the light propagates from $z = 0$ to $z = +\infty$, the detuning $\Delta\beta_{31}(z)$ satisfies another condition $\Delta\beta_{31}(z) = 2\Delta\beta_{21}(z)$. Therefore, the light evolution will first follow the ‘‘eigenstates’’ in Eq. (5) when it is propagating in the left half of the waveguide structure. If the light is propagating in the right half of the waveguide structure, it will adiabatically follow the ‘‘eigenstates’’ in Eq. (7).

When the light propagates from the inputs to $z = 0$, the mixing angle γ in Eq. (5) will evolve from $\frac{\pi}{2}$ to $\frac{\pi}{4}$. This leads to the evolutions of the ‘‘eigenstates’’ that

$$\begin{aligned}\Psi_1^+(z) &: \left(\frac{\sqrt{2}}{2}b_1 + \frac{\sqrt{2}}{2}b_3\right) \rightarrow \left(\frac{1}{2}b_1 + \frac{\sqrt{2}}{2}b_2 + \frac{1}{2}b_3\right) \\ \Psi_1(z) &: \frac{\sqrt{2}}{2}b_1 - \frac{\sqrt{2}}{2}b_3 \\ \Psi_1^-(z) &: -b_2 \rightarrow \left(\frac{1}{2}b_1 - \frac{\sqrt{2}}{2}b_2 + \frac{1}{2}b_3\right).\end{aligned}\quad (11)$$

During the light propagation from $z = 0$ to the outputs, the mixing angle θ in Eq. (7) will evolve from $\frac{\pi}{2}$ to 0, while φ will evolve from $\frac{\pi}{4}$ to 0. Correspondingly, the ‘‘eigenstates’’ in Eq. (7) follows

$$\begin{aligned}\Psi_2^+(z) &: \left(\frac{1}{2}b_1 + \frac{\sqrt{2}}{2}b_2 + \frac{1}{2}b_3\right) \rightarrow b_3 \\ \Psi_2(z) &: \left(\frac{\sqrt{2}}{2}b_1 - \frac{\sqrt{2}}{2}b_3\right) \rightarrow b_2 \\ \Psi_2^-(z) &: \left(-\frac{1}{2}b_1 + \frac{\sqrt{2}}{2}b_2 - \frac{1}{2}b_3\right) \rightarrow -b_1.\end{aligned}\quad (12)$$

If the light is initially incident into WG2, the evolution will first follow the adiabatic state $\Psi_1^-(z)$ and then $\Psi_2^-(z)$ based on the expressions in Eqs. (11) and (12). Therefore, we can predict a complete switch of light from WG2 to WG1. During the process, part of the light will be coupled into

WG3. When the light starts to propagate from WG1 (WG3), it can be considered as a superposition of the adiabatic states $\Psi_1^+(z)$ and $\Psi_1(z)$, which is $b_1 = \frac{\sqrt{2}}{2}[\Psi_1^+(z) + \Psi_1(z)]$ ($b_3 = \frac{\sqrt{2}}{2}[\Psi_1^+(z) - \Psi_1(z)]$). Under the adiabatic condition, the adiabatic states will evolve independently following $\Psi_1^+(z)$ and $\Psi_1(z)$ in the left half of the waveguide structure. From $z = 0$ to the outputs, the adiabatic states will evolve independently following $\Psi_2^+(z)$ and $\Psi_2(z)$. Finally, we can obtain the light distribution with the form $\frac{\sqrt{2}}{2}(b_2 + b_3)$ ($\frac{\sqrt{2}}{2}(b_3 - b_2)$), which implies a one-to-two beam splitting with equal intensity.

2. Linear decrease of detuning $\Delta\beta_{21}(z)$

Suppose the detuning $\Delta\beta_{21}(z)$ is linearly decreased along the propagation direction, which is $\Delta\beta_{21}(z) = -\alpha z$, we find in this case that the evolutions of all mixing angles and ‘‘eigenstates’’ are just opposite to those when $\Delta\beta_{21}(z) = \alpha z$. The detuning $\Delta\beta_{31}(z)$ will first satisfy $\Delta\beta_{31}(z) = 2\Delta\beta_{21}(z)$ in the left half of the waveguide structure, then the condition is fulfilled $\Delta\beta_{31}(z) = 0$ in the right half of the structure. Therefore, the light evolution will firstly obey one of the ‘‘eigenstates’’ in Eq. (7),

$$\begin{aligned}\Psi_2^+(z) &: b_3 \rightarrow \left(\frac{1}{2}b_1 + \frac{\sqrt{2}}{2}b_2 + \frac{1}{2}b_3\right) \\ \Psi_2(z) &: b_2 \rightarrow \left(\frac{\sqrt{2}}{2}b_1 - \frac{\sqrt{2}}{2}b_3\right) \\ \Psi_2^-(z) &: -b_1 \rightarrow \left(-\frac{1}{2}b_1 + \frac{\sqrt{2}}{2}b_2 - \frac{1}{2}b_3\right),\end{aligned}\quad (13)$$

when the light starts to propagate from $z = -\infty$ to $z = 0$. During the process, the mixing angle θ in Eq. (7) evolves from 0 to $\frac{\pi}{2}$ while φ evolves from 0 to $\frac{\pi}{4}$.

When the light continues to propagate from $z = 0$ to $z = +\infty$, it will evolve following one of the ‘‘eigenstates’’ in Eq. (5), which are

$$\begin{aligned}\Psi_1^+(z) &: \left(\frac{1}{2}b_1 + \frac{\sqrt{2}}{2}b_2 + \frac{1}{2}b_3\right) \rightarrow \left(\frac{\sqrt{2}}{2}b_1 + \frac{\sqrt{2}}{2}b_3\right) \\ \Psi_1(z) &: \frac{\sqrt{2}}{2}b_1 - \frac{\sqrt{2}}{2}b_3 \\ \Psi_1^-(z) &: \left(\frac{1}{2}b_1 - \frac{\sqrt{2}}{2}b_2 + \frac{1}{2}b_3\right) \rightarrow -b_2,\end{aligned}\quad (14)$$

with the mixing angle γ evolves from $\frac{\pi}{4}$ to $\frac{\pi}{2}$.

The opposite evolutions of the ‘‘eigenstates’’ given in Eqs. (13) and (14) to those in Eqs. (11) and (12) result in quite different light dynamics in the waveguide structure. If the light is initially incident into WG1, it will totally come out from WG2 although part of the light is coupled into WG3 during the propagation. This can be obtained by observing the adiabatic states $\Psi_2^-(z)$ and $\Psi_1^-(z)$. When the light is incident into WG2 (WG3) at the inputs, it will come out from WG1 and WG3 with the same intensity, following the adiabatic states $\Psi_2(z)$ ($\Psi_2^+(z)$) and $\Psi_1(z)$ ($\Psi_1^+(z)$). Therefore, we can observe complete light transfer and one-to-two beam splitting simultaneously in the waveguide structure under the current choice of the two detunings.

In the situation that either one of the two detunings can have a sign flip, there are still many other choices. We can assume $\Delta\beta_{32}(z) = -|\alpha z|$ and $\Delta\beta_{21}(z) = \pm\alpha z$. Except for this, we can also assume that $\Delta\beta_{32}(z)$ have a sign flip while $\Delta\beta_{21}(z)$ does not, which is $\Delta\beta_{32}(z) = \pm\alpha z$ and $\Delta\beta_{21}(z) = \pm|\alpha z|$. However, a closer look at these choices shows that we do not need to discuss them because they give similar light evolutions in the waveguide structure to what we discussed when $\Delta\beta_{32}(z) = |\alpha z|$ and $\Delta\beta_{21}(z) = \pm\alpha z$.

C. No sign flips in both of the two detunings

The last situation of the two longitudinally varying detunings is that both of them have no sign flips, which is $\Delta\beta_{32}(z) = \pm|\alpha z|$ and $\Delta\beta_{21}(z) = \pm|\alpha z|$. Similar to the above discussions, the two detunings without sign flips can have the same or the opposite variations. Since the two choices may result in different evolutions of light, we should treat them separately.

1. Same variations of the two detunings

Suppose the two detunings without sign flips have the same variations, which can be written as $\Delta\beta_{32}(z) = \Delta\beta_{21}(z) = \pm|\alpha z|$, then the detuning between WG1 and WG3 will always satisfy the condition $\Delta\beta_{31}(z) = 2\Delta\beta_{21}(z)$. Therefore, the evolution of light will follow the “eigenstates” in Eq. (7) under the adiabatic condition.

We can take $\Delta\beta_{32}(z) = \Delta\beta_{21}(z) = |\alpha z|$ as an example for the analysis. When the light starts to propagate from the inputs to the outputs through $z = 0$, the evolutions of the two mixing angles θ and φ in Eq. (7) are $0 \rightarrow \frac{\pi}{2} \rightarrow 0$ and $0 \rightarrow \frac{\pi}{4} \rightarrow 0$, respectively. The corresponding evolutions of the “eigenstates” are

$$\begin{aligned}\Psi_2^+(z) : b_3 &\rightarrow \left(\frac{1}{2}b_1 + \frac{\sqrt{2}}{2}b_2 + \frac{1}{2}b_3\right) \rightarrow b_3 \\ \Psi_2(z) : b_2 &\rightarrow \left(\frac{\sqrt{2}}{2}b_1 - \frac{\sqrt{2}}{2}b_3\right) \rightarrow b_2 \\ \Psi_2^-(z) : -b_1 &\rightarrow \left(-\frac{1}{2}b_1 + \frac{\sqrt{2}}{2}b_2 - \frac{1}{2}b_3\right) \rightarrow -b_1.\end{aligned}\quad (15)$$

It is clear from Eq. (15) that we can always predict complete light return in this case, no matter which individual waveguide is initially incident into. During the propagation, the light in one waveguide will be coupled into its neighboring waveguides.

As for the choice of the two detunings $\Delta\beta_{32}(z) = \Delta\beta_{21}(z) = -|\alpha z|$, it also leads to the prediction of complete light return, regardless the incidence of the light at the inputs.

2. Opposite variations of the two detunings

If the two longitudinally varying detunings without sign flips have opposite variations, which corresponds to $\Delta\beta_{32}(z) = -\Delta\beta_{21}(z) = \pm|\alpha z|$, we find that the condition $\Delta\beta_{31}(z) = 0$ is fulfilled. Thus, the light will propagate following the “eigenstates” in Eq. (5).

We can take $\Delta\beta_{32}(z) = -\Delta\beta_{21}(z) = |\alpha z|$ as an instance for the analysis. During the propagation of light from $z = -\infty$ to $z = +\infty$ through $z = 0$, the mixing angle γ in Eq. (5) will

evolve following $\frac{\pi}{2} \rightarrow \frac{\pi}{4} \rightarrow \frac{\pi}{2}$ while the “eigenstates” will evolve based on

$$\begin{aligned}\Psi_1^+(z) : \left(\frac{\sqrt{2}}{2}b_1 + \frac{\sqrt{2}}{2}b_3\right) &\rightarrow \left(\frac{1}{2}b_1 + \frac{\sqrt{2}}{2}b_2 + \frac{1}{2}b_3\right) \\ &\rightarrow \left(\frac{\sqrt{2}}{2}b_1 + \frac{\sqrt{2}}{2}b_3\right) \\ \Psi_1(z) : \frac{\sqrt{2}}{2}b_1 - \frac{\sqrt{2}}{2}b_3 & \\ \Psi_1^-(z) : -b_2 &\rightarrow \left(\frac{1}{2}b_1 - \frac{\sqrt{2}}{2}b_2 + \frac{1}{2}b_3\right) \rightarrow -b_2.\end{aligned}\quad (16)$$

In this case, we can find complete light return if it is initially incident into WG2, as described by the adiabatic state $\Psi_1^-(z)$. If the light is incident into WG1 at the inputs, it can be considered as a superposition of the adiabatic states $\Psi_1^+(z)$ and $\Psi_1(z)$, which is $b_1 = \frac{\sqrt{2}}{2}[\Psi_1^+(z) + \Psi_1(z)]$. After the independent evolutions of the two adiabatic states under the adiabatic condition, finally we can still obtain complete light return in WG1. The phenomenon is the same if the light starts to propagate from WG3. However, we note that the prediction actually fails under the incidence of light into WG1 or WG3, which will be explained in detail in the following section.

As for the case $\Delta\beta_{32}(z) = -\Delta\beta_{21}(z) = -|\alpha z|$, the light evolution is the same as that when $\beta_{32}(z) = -\Delta\beta_{21}(z) = |\alpha z|$ and we do not show it here.

III. NUMERICAL CALCULATIONS

In the framework of double RAP, the above theoretical analysis has predicted light splitting, complete light transfer, or complete light return under different choices of the two spatially varying detunings. In this section, we are going to carry out numerical calculations to demonstrate the above analysis. First, we will directly solve the coupled mode equations Eq. (3) to verify the theoretical predictions. Afterward, we will optically simulate the propagation of light in waveguides with designed parameters according to the calculation results of Eq. (3).

When solving the coupled mode equations Eq. (3), we will make use of the fourth-order Runge-Kutta method. During the calculations, the two identical coupling constants between adjacent waveguides are supposed to be with Gaussian shapes, which are $C_{32}(z) = C_{21}(z) = C_0 \exp(-\ln 4z^2/z_0^2)$ with C_0 the amplitude of the coupling constant and z_0 the full width at half maximum of the Gaussian coupling-constant pulse. The assumption is consistent with that in theoretical analysis. At the inputs and outputs of the waveguide structure, the couplings can be ignored. At the central position $z = 0$, the couplings reach their maximum. In the calculations, all the parameters are chosen with respect to z_0 . The amplitude of the coupling constant is fixed at $C_0 = 50/z_0$, while the positive “linear chirp rate” of the two detunings is fixed at $\alpha = 10/z_0^2$.

The optical analog of the double RAP is carried out in planar waveguides in the xz plane based on the calculation results of Eq. (3). We are going to employ the BPM method [32], which has been widely used to design optical

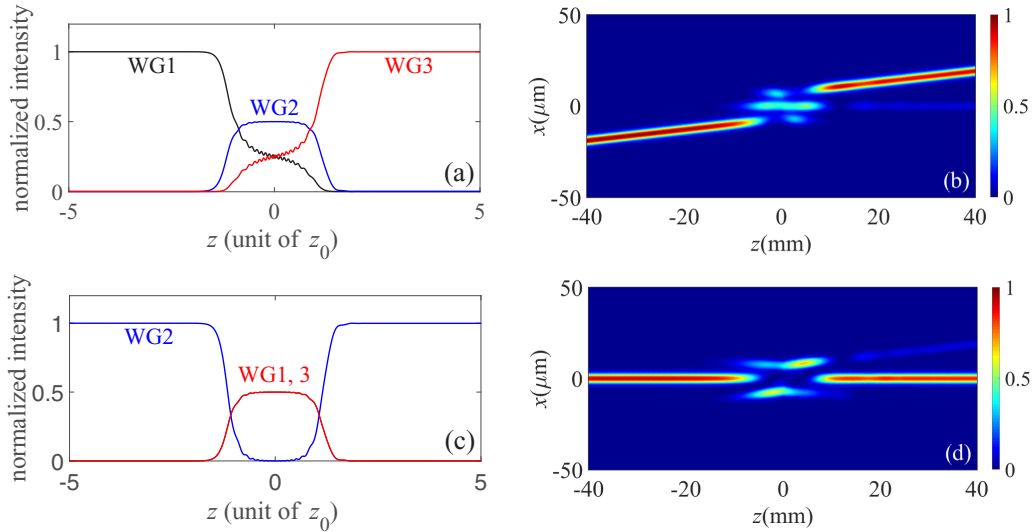


FIG. 2. Evolution of light when $\Delta\beta_{32}(z) = \Delta\beta_{21}(z) = \alpha z$. (a) and (c) are obtained by solving Eq. (3) while (b) and (d) are the optical simulations in waveguides. During the light propagation, Δn_1 decreases following $0.001 \rightarrow 0.0008 \rightarrow 0.0005$ while Δn_3 increases following $0.0005 \rightarrow 0.0008 \rightarrow 0.001$. The distances shown in Fig. 1(b) are $d_1 = d_4 = 14 \mu\text{m}$ and $d_2 = d_3 = 10 \mu\text{m}$.

waveguides and predict the light evolution in such structures. In the optical simulations, straight waveguides instead of curved ones are used to mimic the Gaussian-type coupling constants for simplicity, which is due to the reason that $C_{jm}(z)$ decreases nearly exponentially with the distance between waveguides d . As to the space-dependent detunings $\Delta\beta_{jm}(z)$, they can be approximately realized by linearly modifying the refractive indices of the waveguides along the propagation direction. Experimentally, reconfigurable photoinduced waveguides on a $\text{Sr}_x\text{Ba}_{1-x}\text{Nb}_2\text{O}_6$ (SBN) crystal with $x = 0.61$ are good candidates for this purpose [6,33]. The combination of a local illumination by the control beam and the electric field applied to the SBN crystal can lead to a local modification of the refractive index of the crystal.

During the optical simulations, the refractive index of the substrate is chosen as $n_s = 2.3109$. The widths and lengths of the three waveguides are fixed at $5 \mu\text{m}$ and 80mm , respectively. The wavelength of the incident light is $\lambda = 633 \text{nm}$. The refractive index contrast of WG2 with respect to n_s is kept unchanged at $\Delta n_2 = 0.0008$ while those of the other two waveguides, Δn_1 and Δn_3 , are linearly varied along the propagation direction. However, the refractive index contrasts of WG1 and WG3 at the position $z = 0$ are always set equal to Δn_2 , which is $\Delta n_1(z = 0) = \Delta n_3(z = 0) = 0.0008$. This guarantees that the two detunings are zero at this position. As to the distances between the three waveguides, they are supposed to be minimum at the same position $z = 0$, which is $d_0 = 2 \mu\text{m}$. Therefore, the corresponding maximum couplings of the three waveguides are estimated to be $C_0 \approx 0.4 \text{mm}^{-1}$. This is done by observing light oscillation between two identical parallel waveguides with their refractive index contrasts equal to 0.0008 . The maximum coupling is obtained by calculating the coupling length L according to the relation $C_0 = \frac{\pi}{2L}$.

In the following, we are going to give the calculation results with respect to different choices of the two spatially

varying detunings. Note that only those choices which are analyzed in detail in Sec. II are numerically calculated.

A. Sign flips in both of the two detunings

We first carry out the calculations in the situation that both of the two longitudinally varying detunings have sign flips. Same as the discussions in Sec. II, light evolutions are calculated separately when the two detunings have the same or the opposite variations along the propagation direction.

If the two detunings vary the same by assuming $\Delta\beta_{32}(z) = \Delta\beta_{21}(z) = \alpha z$, then the refractive index contrast of WG1, Δn_1 , is set linearly decreased from 0.001 to 0.0008 in the left half of the waveguide structure. After the light passes through the central position $z = 0$, Δn_1 continues to decrease linearly from 0.0008 to 0.0005 . Correspondingly, the refractive index contrast of WG3, Δn_3 , increases following $0.0005 \rightarrow 0.0008 \rightarrow 0.001$ during the light propagation through $z = 0$. Under the choices of Δn_1 and Δn_3 , the linear increases of the two detunings, $\Delta\beta_{32}(z)$ and $\Delta\beta_{21}(z)$, can be approximately realized in the waveguide structure. The absolute values of the two detunings at the inputs and outputs are close to each other and they are the maximum, which are estimated to be $\Delta\beta_{jm}^{\text{max}} \approx 1.69 \text{mm}^{-1}$. This is done by calculating the propagation constants of the waveguides $\beta_j = n_{\text{eff}}^j k_0$ ($j = 1, 2, 3$) with their refractive index contrasts fixed at 0.001 , 0.0008 , and 0.0005 , respectively. In this expression, n_{eff}^j is the effective refractive index while $k_0 = 2\pi/\lambda$ is the wave number. The distances between the three waveguides at the inputs and outputs are set to be $d_1 = d_4 = 14 \mu\text{m}$ and $d_2 = d_3 = 10 \mu\text{m}$. Calculation results by solving Eq. (3) and optical simulations based on the BPM method are displayed in Fig. 2.

Figures 2(a) and 2(c) are the direct calculations of Eq. (3). In Fig. 2(a), we can find that light is completely switched from WG1 to WG3 through the intermediate waveguide. At $z = 0$, half of the light intensity is coupled into WG2 while the other half is equally distributed in WG1 and WG3. We

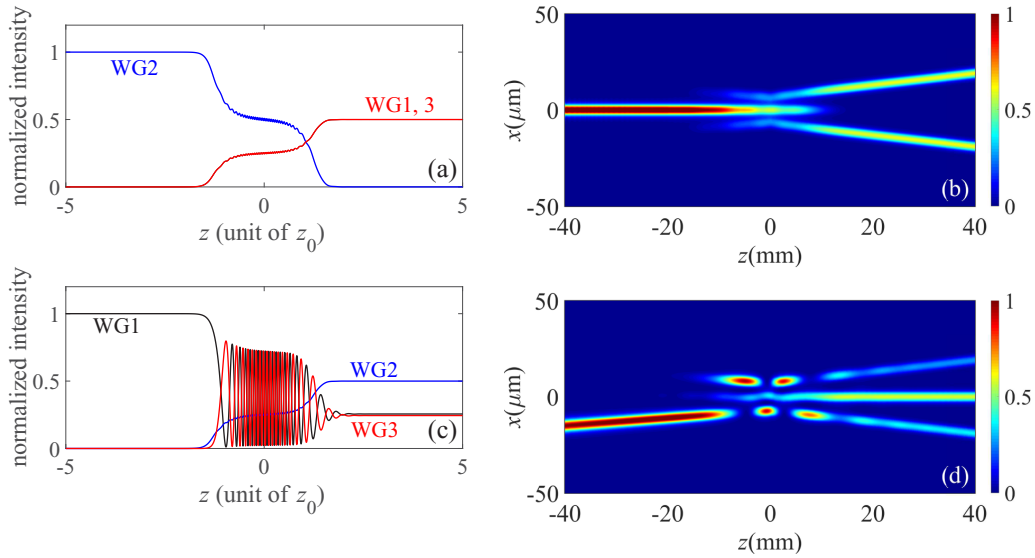


FIG. 3. Similar to Fig. 2 but with $\Delta\beta_{32}(z) = -\Delta\beta_{21}(z) = \alpha z$. Both Δn_1 and Δn_3 are increased following $0.0005 \rightarrow 0.0008 \rightarrow 0.001$ during the light propagation. The four distances are $d_1 = d_3 = 10 \mu\text{m}$ and $d_2 = d_4 = 14 \mu\text{m}$.

can also find a similar light switch from WG3 to WG1 and the result is not shown here. When the light propagation starts from WG2, it is found that it will still come out from this waveguide, as shown in Fig. 2(c). At $z = 0$, all the light will be equally coupled into WG1 and WG3. These calculation results are exactly the same as those predictions in the above analysis. Figures 2(b) and 2(d) are the corresponding optical analogs of Figs. 2(a) and 2(c) in waveguides. The simulations are also in good agreement with the calculation results based on Eq. (3). Therefore, we find that we can simultaneously observe complete light transfer and complete light return in the waveguide structure.

If the two detunings vary the opposite by assuming $\Delta\beta_{32}(z) = -\Delta\beta_{21}(z) = \alpha z$, then the refractive index contrasts of WG1 and WG3, Δn_1 and Δn_3 , are set to increase following $0.0005 \rightarrow 0.0008 \rightarrow 0.001$ from the inputs to the outputs through $z = 0$. The distances between the waveguides at the inputs and outputs are set as $d_1 = d_3 = 10 \mu\text{m}$ and $d_2 = d_4 = 14 \mu\text{m}$. The calculations based on Eq. (3) and the corresponding optical simulations are shown in Fig. 3.

We can see from Fig. 3(a) that all the light which is initially incident into WG2 will be adiabatically coupled into WG1 and WG3 with the same intensity. When the light starts to propagate from WG1, we can also obtain a light splitting with

half of the total intensity coming out of WG2 while the left is equally distributed in WG1 and WG3, as shown in Fig. 3(c). If the light is initially incident into WG3, the evolution is the same as that in Fig. 3(c) and we do not show it here. These calculations are consistent with the above theoretical analysis. The optical simulations in waveguides displayed in Figs. 3(b) and 3(d) also agree well with the results in Figs. 3(a) and 3(c).

In Figs. 3(c) and 3(d), the light evolution looks non-adiabatic due to the rapid oscillation of light between WG1 and WG3. We can simply demonstrate the adiabaticity by calculating the light intensity coming out of one of the three waveguides under variations of the coupling constant amplitude C_0 and the positive “linear chirp rate” α . For instance, light coming out of WG3 under variations of C_0 and α is given in Fig. 4(a). It is clear from this figure that the light intensity coming out of WG3 is stable under fluctuations of the two parameters as long as they are strong enough to satisfy the adiabatic condition. Furthermore, we can also verify the adiabaticity by the evolutions of the eigenvalues in Fig. 4(b). Since $b_1 = \frac{\sqrt{2}}{2}[\Psi_1(z) + \Psi_1^-(z)]$ at the inputs based on the analysis, we should focus on the evolutions of the two corresponding eigenvalues ϵ_1 and ϵ_1^- . We can see from Fig. 4(b) that the two eigenvalues do not cross any more after they separate

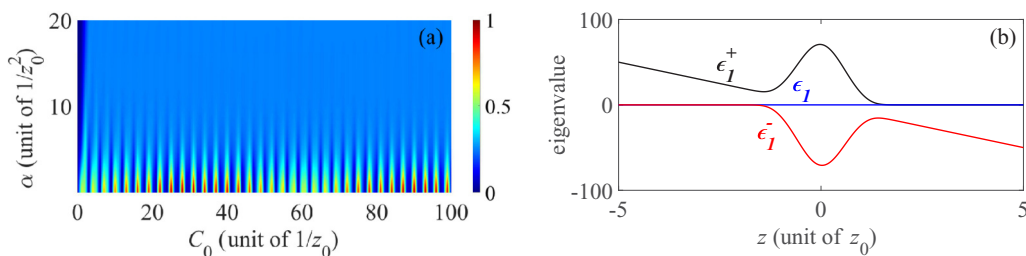


FIG. 4. (a) Light coming out of WG3 under variations of the coupling constant amplitude C_0 and the positive “linear chirp rate” α , and (b) evolutions of the eigenvalues in the case of Fig. 3(c).

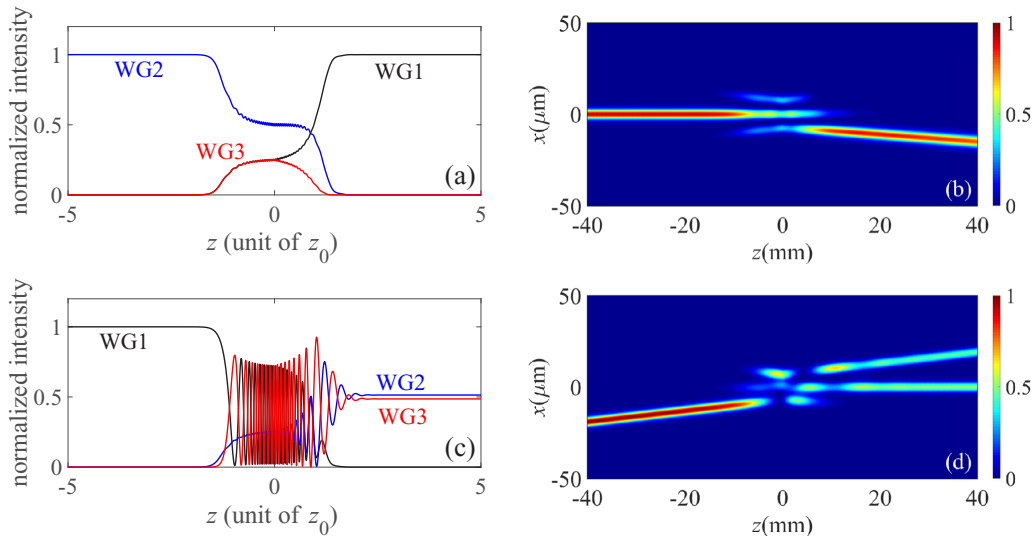


FIG. 5. Similar to Fig. 2 but with $\Delta\beta_{32}(z) = |\alpha z|$ and $\Delta\beta_{21}(z) = \alpha z$. During the light propagation, Δn_1 decreases following $0.001 \rightarrow 0.0008 \rightarrow 0.0005$ while Δn_3 varies following $0.001 \rightarrow 0.0008 \rightarrow 0.001$. The four distances are $d_1 = d_3 = d_4 = 14 \mu\text{m}$ and $d_2 = 10 \mu\text{m}$.

at the inputs. Therefore, the two adiabatic states $\Psi_1(z)$ and $\Psi_1^-(z)$ will evolve independently and the adiabaticity is well preserved.

B. Sign flip in either one of the two detunings

For the situation that there is a sign flip in either one of the two detunings, we will carry out the numerical calculations by choosing $\Delta\beta_{32}(z) = |\alpha z|$ and $\Delta\beta_{21}(z) = \pm\alpha z$ according to the analysis in Sec. II. The results are given separately when the detuning $\Delta\beta_{21}(z)$ is linearly increased or decreased.

When $\Delta\beta_{21}(z) = \alpha z$, the refractive index contrast of WG1, Δn_1 , is set to decrease following $0.001 \rightarrow 0.0008 \rightarrow 0.0005$ during the light propagation through $z = 0$. As to that of WG3, Δn_3 , it is linearly decreased from 0.001 to 0.0008 in the left half of the waveguide structure. After the light passes through the central position, it starts to increase linearly from 0.0008 to 0.001. The distances between the waveguides at the inputs and outputs are $d_1 = d_3 = d_4 = 14 \mu\text{m}$ and $d_2 = 10 \mu\text{m}$. The calculation results and the corresponding optical simulations are presented in Fig. 5.

We can clearly see from Fig. 5(a) that, light will be completely transferred into WG1 when it is initially incident into WG2. If the light starts to propagate from WG1 (WG3), it will always come out from WG2 and WG3 with the same intensity.

In Fig. 5(c), we only present the light evolution starting from WG1. The calculations are the same as the theoretical predictions. The corresponding classical analogs in Figs. 5(b) and 5(d) are accordant with the calculations in Figs. 5(a) and 5(c).

Since the light evolution looks nonadiabatic due to the rapid oscillations in Figs. 5(c) and 5(d), we again give a contour plot of the light intensity coming out of WG3 under variations of C_0 and α to demonstrate the adiabaticity, which is shown in Fig. 6(a). We can see from this figure that the light intensity out from WG3 is still stable against fluctuations of C_0 and α . The evolutions of the eigenvalues in Fig. 6(b) also verify the adiabaticity. Since $b_1 = \frac{\sqrt{2}}{2}[\Psi_1^+(z) + \Psi_1(z)]$ at the inputs, we should first focus on the evolutions of eigenvalues ϵ_1^+ and ϵ_1 . After the light passes through the central position, the two eigenvalues will start to evolve along ϵ_2^+ and ϵ_2 . It is clear from Fig. 6(b) that the two eigenvalues will not cross anymore after they separate at the inputs. Therefore, the corresponding adiabatic states can evolve independently and the adiabaticity is preserved.

When $\Delta\beta_{21}(z) = -\alpha z$, it corresponds that the detuning $\Delta\beta_{21}(z)$ is linearly decreased along the propagation direction. In this case, the refractive index contrast of WG1, Δn_1 , is set to increase following $0.0005 \rightarrow 0.0008 \rightarrow 0.001$ while the variation of Δn_3 is the same as that in the case of $\Delta\beta_{21}(z) = \alpha z$ during the light propagation through $z = 0$. The distances

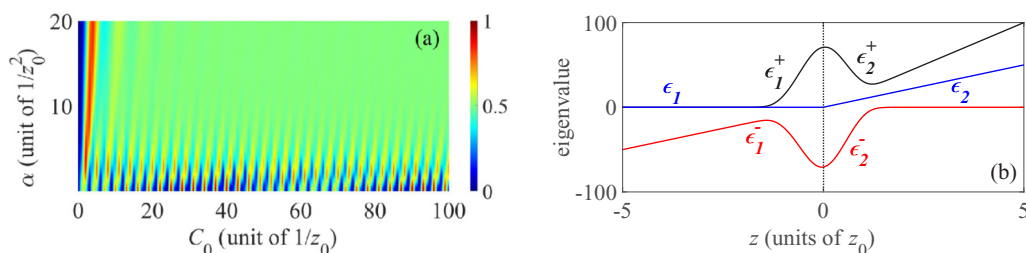


FIG. 6. (a) Light coming out of WG3 under variations of the coupling constant amplitude C_0 and the positive “linear chirp rate” α , and (b) evolutions of the eigenvalues in the case of Fig. 5(c).

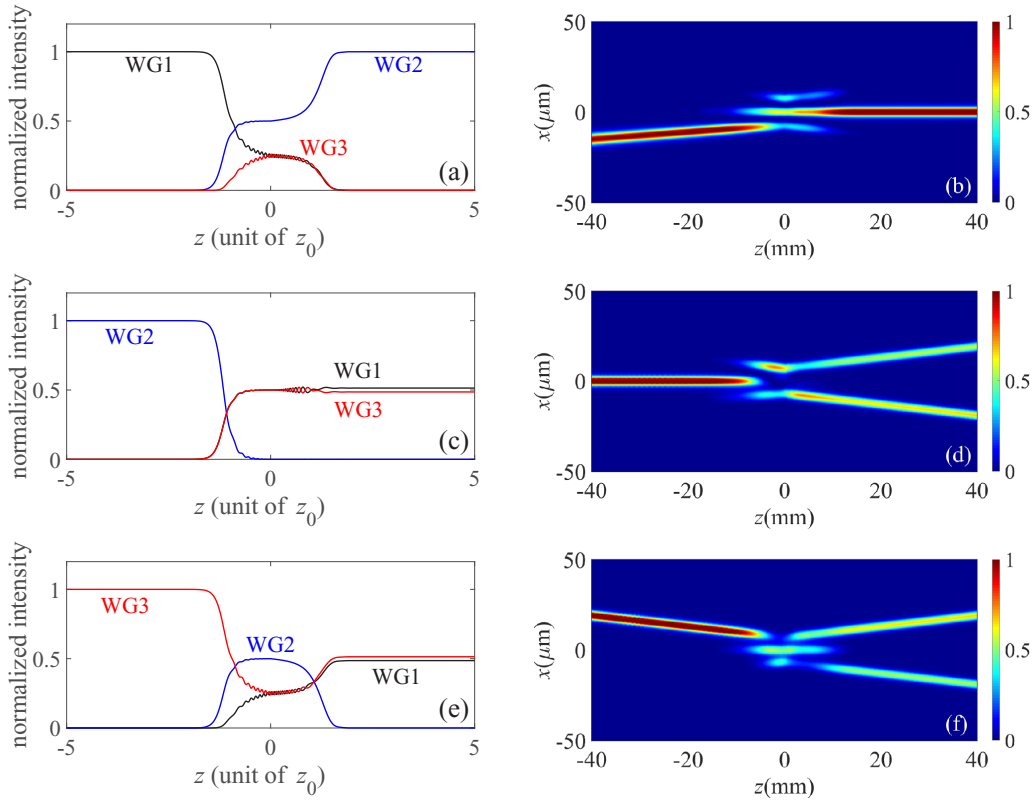


FIG. 7. Similar to Fig. 2 but with $\Delta\beta_{32}(z) = |\alpha z|$ and $\Delta\beta_{21}(z) = -\alpha z$. During the light propagation, Δn_1 increases following $0.0005 \rightarrow 0.0008 \rightarrow 0.001$ while Δn_3 varies following $0.001 \rightarrow 0.0008 \rightarrow 0.001$. The four distances are $d_1 = 10 \mu\text{m}$ and $d_2 = d_3 = d_4 = 14 \mu\text{m}$.

between the waveguides at the inputs and outputs are set to be $d_1 = 10 \mu\text{m}$ and $d_2 = d_3 = d_4 = 14 \mu\text{m}$. Results including the calculations based on Eq. (3) and the optical simulations in waveguides are given in Fig. 7.

If the light is initially incident into WG1, we can find from Fig. 7(a) that it will be completely transferred into WG2.

However, WG3 still takes part into the coupling during the evolution of light. If the light starts to propagate from WG2 or WG3, we will find the appearance of light splitting. The light will always come out from WG1 and WG3 with equal intensity, as displayed in Figs. 7(c) and 7(e). These calculation results based on Eq. (3) are exactly the same as the theoretical

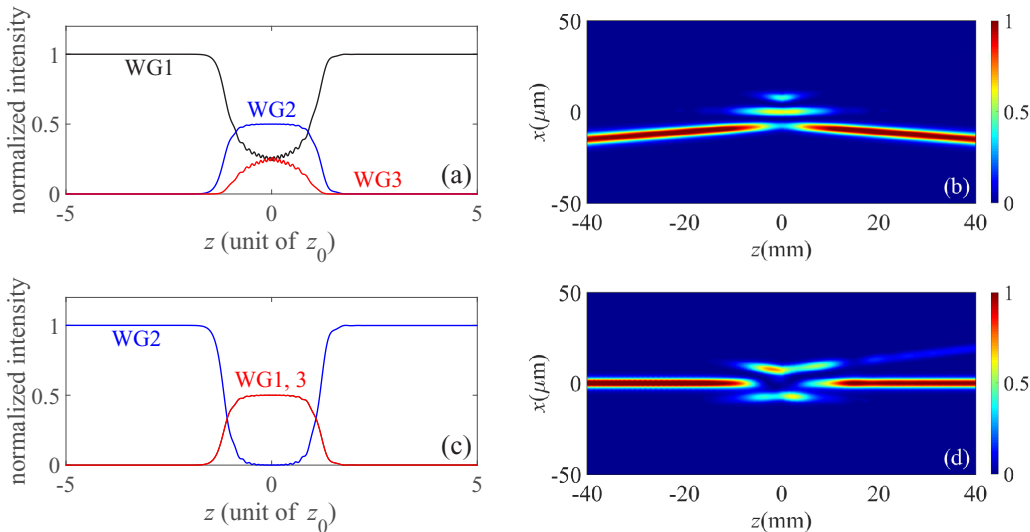


FIG. 8. Similar to Fig. 2 but with $\Delta\beta_{32}(z) = \Delta\beta_{21}(z) = |\alpha z|$. During the light propagation, the variations of Δn_1 and Δn_3 follow $0.0005 \rightarrow 0.0008 \rightarrow 0.0005$ and $0.001 \rightarrow 0.0008 \rightarrow 0.001$, respectively. The four distances are $d_1 = d_2 = 10 \mu\text{m}$ and $d_3 = d_4 = 14 \mu\text{m}$.

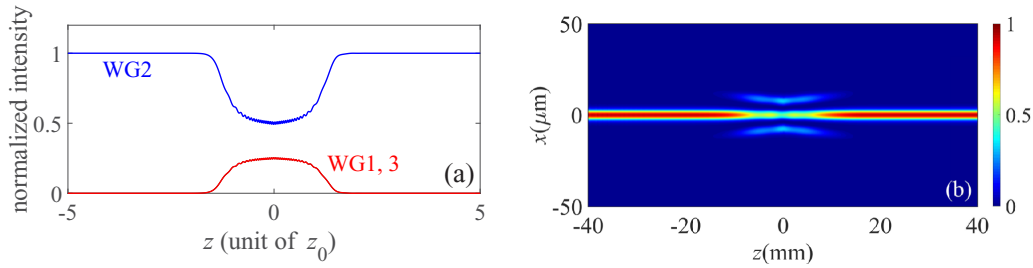


FIG. 9. Similar to Fig. 2 but with $\Delta\beta_{32}(z) = -\Delta\beta_{21}(z) = |\alpha z|$. During the light propagation, the variations of Δn_1 and Δn_3 follow $0.001 \rightarrow 0.0008 \rightarrow 0.001$. The four distances are $d_1 = d_2 = d_3 = d_4 = 14 \mu\text{m}$.

predictions. Still, the corresponding optical simulations agree very well with the results in Figs. 7(a), 7(c), and 7(e), as can be found in Figs. 7(b), 7(d), and 7(f). In this case, we find that we can observe light splitting and complete light transfer simultaneously in the waveguide structure.

C. No sign flips in both of the two detunings

The last possibility of the two longitudinally varying detunings is that they both have no sign flips while they vary the same or the opposite. According to the theoretical analysis, we will calculate the light evolutions in the case of $\Delta\beta_{32}(z) = \Delta\beta_{21}(z) = |\alpha z|$ and $\Delta\beta_{32}(z) = -\Delta\beta_{21}(z) = |\alpha z|$, respectively.

If the two detunings without sign flips have the same variations, which is $\Delta\beta_{32}(z) = \Delta\beta_{21}(z) = |\alpha z|$, then the refractive index contrast of WG1, Δn_1 , will vary following $0.0005 \rightarrow 0.0008 \rightarrow 0.0005$ during the light propagation. As to the variation of Δn_3 , it will follow $0.001 \rightarrow 0.0008 \rightarrow 0.001$. The distances between the waveguides at the inputs and outputs are set to be $d_1 = d_2 = 10 \mu\text{m}$ and $d_3 = d_4 = 14 \mu\text{m}$. The calculation results based on Eq. (3) and the corresponding optical simulations are illustrated in Fig. 8.

In this figure, either the calculations from Eq. (3) or the optical simulations clearly show that we will always observe complete light return in this case, no matter which waveguide is initially incident into. Besides, the neighboring waveguides will be involved into the coupling during the light propagation. When the light starts to propagate from WG3, the evolution is similar to that in Fig. 8(a) and we do not present it here. All the results in Fig. 8 are consistent with the theoretical predictions in Sec. II.

If the two detunings without sign flips have the opposite variations, which is $\Delta\beta_{32}(z) = -\Delta\beta_{21}(z) = |\alpha z|$, then both

of the two refractive index contrasts of WG1 and WG3, Δn_1 and Δn_3 , will vary the same following $0.001 \rightarrow 0.0008 \rightarrow 0.001$. The distances between the waveguides at the inputs and outputs are also the same, which are $d_1 = d_2 = d_3 = d_4 = 14 \mu\text{m}$. The corresponding calculation results are given in Fig. 9.

In this figure, we can observe complete light return when the light is initially incident into WG2. During the propagation, the two neighboring waveguides WG1 and WG3 take part in the coupling. The calculation results still agree with theoretical predictions. However, we note that the light evolution is nonadiabatic if it is incident into WG1 (WG3) at the inputs. The calculation results are contrary to the theoretical analysis in Sec. II C that there will be a complete light return. The nonadiabatic light evolution is clear by calculating the light coming out of WG1 under variations of C_0 and α if it starts to propagate from this waveguide, which is depicted in Fig. 10(a). We can see from this figure that light intensity coming out of WG1 is quite sensitive to the two parameters, indicating the nonadiabaticity of the light evolution. The failure of the prediction in Sec. II C can be explained by the evolutions of the eigenvalues in Fig. 10(b). Since $b_1 = \frac{\sqrt{2}}{2}[\Psi_1^+(z) + \Psi_1(z)]$ at the inputs, we can see from this figure that the corresponding two eigenvalues ϵ_1^+ and ϵ_1^- will coincide with each other again during the propagation. Therefore, the two adiabatic states $\Psi_1^+(z)$ and $\Psi_1(z)$ cannot evolve independently and the adiabaticity is not preserved.

The numerical demonstrations of the adiabatic light evolution indicate that the double RAP is robust in most of the cases mentioned above, which is similar to the other adiabatic passages [9,12–17]. The robustness of the double RAP promises possible applications of the technique in designing devices such as achromatic beam splitter or beam coupler. The

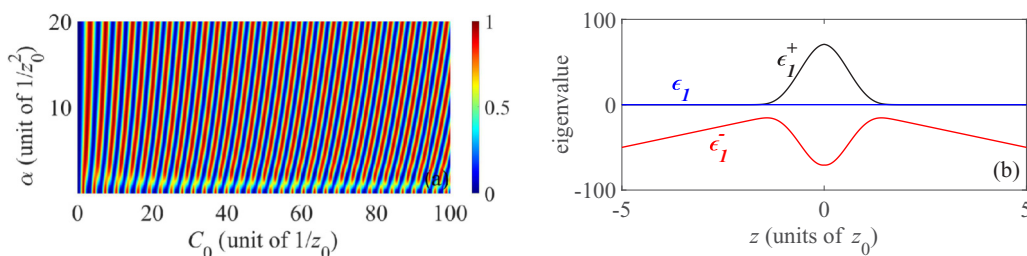


FIG. 10. (a) Light coming out of WG1 under variations of the coupling constant amplitude C_0 and the positive “linear chirp rate” α , and (b) evolutions of the eigenvalues when the light is initially incident into WG1 in the case of $\Delta\beta_{32}(z) = -\Delta\beta_{21}(z) = |\alpha z|$.

devices can even possess the two functionalities simultaneously without adjusting the parameters.

IV. CONCLUSIONS

To conclude, we have investigated the classical analog of a quantum control technique, the double RAP, in three evanescently coupled waveguides. The two detunings between the waveguides are supposed to be space dependent and they can have sign flips or not when they tend to zero. Both the theoretical analysis and numerical calculations show that beam

splitting, complete light transfer, or complete light return can be observed in the waveguide structure, which is determined by the choice of the two detunings. The technique in optical waveguides can have possible applications in designing devices such as the achromatic beam splitter or beam coupler.

ACKNOWLEDGMENT

This work was supported by the National Natural Science Foundation of China (Grants No. 11974109, No. 11774089, and No. 12034007).

-
- [1] A. Fratilocchi and G. Assanto, *Opt. Express* **14**, 2021 (2006).
 - [2] C. Ciret, M. Alonzo, V. Coda, A. A. Rangelov, and G. Montemezzani, *Phys. Rev. A* **88**, 013840 (2013).
 - [3] M. Mrejen, H. Suchowski, T. Hatakeyama, C. H. Wu, L. Feng, K. O'Brien, Y. Wang, and X. Zhang, *Nat. Commun.* **6**, 7565 (2015).
 - [4] H. Oukraou, V. Coda, A. A. Rangelov, and G. Montemezzani, *Phys. Rev. A* **97**, 023811 (2018).
 - [5] S. Longhi, *Laser Photon. Rev.* **3**, 243 (2009).
 - [6] H. Oukraou, L. Vittadello, V. Coda, C. Ciret, M. Alonzo, A. A. Rangelov, N. V. Vitanov, and G. Montemezzani, *Phys. Rev. A* **95**, 023811 (2017).
 - [7] E. Paspalakis, *Opt. Commun.* **258**, 30 (2006).
 - [8] S. Longhi, *Phys. Rev. E* **73**, 026607 (2006).
 - [9] H. P. Chung, K. H. Huang, S. L. Yang, W. K. Chang, C. W. Wu, F. Setzpfandt, T. Pertsch, D. N. Neshev, and Y. H. Chen, *Opt. Express* **23**, 30641 (2015).
 - [10] F. Dreisow, A. Szameit, M. Heinrich, R. Keil, S. Nolte, A. Tünnermann, and S. Longhi, *Opt. Lett.* **34**, 2405 (2009).
 - [11] G. Della Valle, M. Ornigotti, T. T. Fernandez, P. Laporta, S. Longhi, A. Coppa, and V. Foglietti, *Appl. Phys. Lett.* **92**, 011106 (2008).
 - [12] C. Ciret, V. Coda, A. A. Rangelov, D. N. Neshev, and G. Montemezzani, *Phys. Rev. A* **87**, 013806 (2013).
 - [13] A. A. Rangelov and N. V. Vitanov, *Phys. Rev. A* **85**, 055803 (2012).
 - [14] C. Ciret, V. Coda, A. A. Rangelov, D. N. Neshev, and G. Montemezzani, *Opt. Lett.* **37**, 3789 (2012).
 - [15] K. Chung, T. J. Karle, M. Rab, A. D. Greentree, and S. Tomljenovic-Hanic, *Opt. Express* **20**, 23108 (2012).
 - [16] T. Lunghi, F. Doutra, A. P. Rambur, M. Bellec, M. P. De Micheli, A. M. Apetrei, O. Alibart, N. Belabas, S. Tascu, and S. Tanzilli, *Opt. Express* **26**, 27058 (2018).
 - [17] R. Alrifai, V. Coda, A. A. Rangelov, and G. Montemezzani, *Phys. Rev. A* **100**, 063841 (2019).
 - [18] H. S. Hristova, A. A. Rangelov, G. Montemezzani, and N. V. Vitanov, *Phys. Rev. A* **93**, 033802 (2016).
 - [19] S. Longhi, G. Della Valle, M. Ornigotti, and P. Laporta, *Phys. Rev. B* **76**, 201101(R) (2007).
 - [20] H. C. Chung, S. Martínez-Garaot, X. Chen, J. G. Muga, and S. Y. Tseng, *Europhys. Lett.* **127**, 34001 (2019).
 - [21] S. Y. Tseng and X. Chen, *Opt. Lett.* **37**, 5118 (2012).
 - [22] S. Y. Tseng, R. D. Wen, Y. F. Chiu, and X. Chen, *Opt. Express* **22**, 18849 (2014).
 - [23] X. Chen, R. D. Wen, and S. Y. Tseng, *Opt. Express* **24**, 18322 (2016).
 - [24] S. Martínez-Garaot, S. Y. Tseng, and J. G. Muga, *Opt. Lett.* **39**, 2306 (2014).
 - [25] C. P. Ho and S. Y. Tseng, *Opt. Lett.* **40**, 4831 (2015).
 - [26] S. Martínez-Garaot, J. G. Muga, and S. Y. Tseng, *Opt. Express* **25**, 159 (2017).
 - [27] B. T. Torosov, G. Della Valle, and S. Longhi, *Phys. Rev. A* **89**, 063412 (2014).
 - [28] W. Huang, A. A. Rangelov, and E. Kyoseva, *Phys. Rev. A* **90**, 053837 (2014).
 - [29] W. Huang, L. K. Ang, and E. Kyoseva, *J. Phys. D* **53**, 035104 (2020).
 - [30] W. P. Huang, *J. Opt. Soc. Am. A* **11**, 963 (1994).
 - [31] N. V. Vitanov, M. Fleischhauer, B. W. Shore, and K. Bergmann, *Adv. Atom. Mol. Opt. Phys.* **46**, 55 (2001).
 - [32] K. Kawano and T. Kitoh, *Introduction to Optical Waveguide Analysis: Solving Maxwell's Equations and the Schrödinger Equation* (John Wiley and Sons, New York, 2001).
 - [33] M. Gorram, V. Coda, P. Thévenin, and G. Montemezzani, *Appl. Phys. B* **95**, 565 (2009).